DISCRETE ELEMENT MODELING OF DIKE-INDUCED DEFORMATION. D. Y. Wyrick and K. J. Smart, Department of Earth, Material, and Planetary Sciences, Southwest Research Institute® (6220 Culebra Rd., San Antonio, TX, 78238-5166, USA; dwyrick@swri.org)

Introduction: The Tharsis region of Mars is characterized by large volcanic and tectonic centers with distinct sets of graben systems. Many of the radially oriented grabens have been inferred to form in response to intrusion of magmatic dikes. This interpretation is based primarily upon early physical and numerical (boundary element) models that were developed originally to understand surface deformation associated with dike emplacement on Earth. In this study, we constructed and analyzed two-dimensional discrete element models to test the hypothesis of shallow dike emplacement and widening as a primary mechanism for the production of grabens on Mars. In particular, our models are designed to explore the extent to which a widening subsurface dike under varying emplacement conditions will induce near-surface and surface deformation.

Methodology: The use of discrete element models allows for permanent deformation and material heterogeneity to be simulated. In contrast, boundary element models are limited by an assumption of homogeneous elastic behavior. We performed discrete element modeling of dike-related deformation using the code PFC2D [1]. PFC2D is based on the discrete element method that was developed initially for analyzing the mechanical interaction of granular materials [2]. With the addition of particle bonding, the method has been extended to a variety of problems in solid mechanics, including rock fracturing and seismicity [3,4,5,6,7]. The discrete element formulation requires selection of a set of micromechanical properties (e.g., friction, normal and shear bond stiffness and strength) that describe the interaction of the elastic particles with each other and the model boundaries (see [4], for details on the theoretical framework of PFC). The result is a set of micromechanical properties that provides the correct bulk (macroscale) material behavior, which includes both the elastic (recoverable) and inelastic (non-recoverable) components characteristic of natural deformation.

For all models, stratigraphic material was modeled by generating particles in an initial model area 10 km wide. The particles have a diameter range of 12.8 – 42.9 m scaled to the kilometer scale model boundaries (smaller particle size ranges generate billions of particles which overwhelm the computations). A half model space was used to conserve computation time. The particles are assigned uniform stiffness and friction values throughout the model area. Blue and red colored layering was added for visualization purposes only and does not affect material behavior. Once the model reached equilibrium (no large out-of-balance forces), the simulated dike was widened. The dike was assumed to have reached a neutral buoyancy level (i.e., stopped vertically ascending) 1.25 km below the model surface and widened in place. This depth to dike tip resulted in the most significant surface deformation while still remaining within the range of depths calculated by [8] for non-eruptive dikes. The dike is widened to 1 km in half-width (2 km overall width); although this exceeds the maximum widths calculated for Martian dikes [8], we found that a large dike width was necessary to produce significant surface deformation characteristics. Internal pressures within the dike are ignored and the dike walls are modeled by forcibly widening the dike into the surrounding model space. During model evolution, however, the stress state was calculated in the area adjacent to the dike plane with a horizontal stress magnitude of approximately 127 MPa, consistent with values reported for internal dike pressures [8].

Results: Previous modeling efforts have examined the role of a widening subsurface dike in the absence of regional extension and under various configurations of mechanical layered stratigraphy [9]. For comparison, the base model is presented here as model A. In model A (Figure 1), no bonds are applied to the particles and their behavior is consistent with unconsolidated rock or very weak regolith material. Dike growth produces compressional forces in the material adjacent to the dike plane and a corresponding topographic uplift at the surface, similar to results predicted by previous boundary element models [10,11,12]. Contractional folds are seen in the subsurface, producing surface deformation away from the dike for approximately six times the width of the dike (6.2 km). The topographic peak occurs at approximately twice the width of the underlying dike (1.9 km), and the magnitude of uplift for the unconsolidated regolith model is 0.6 km, corresponding to the topographic relief of the trough. It should be noted that for the unconsolidated model A, the topographic low of the trough immediately above the dike does not drop below the regional topographic surface.

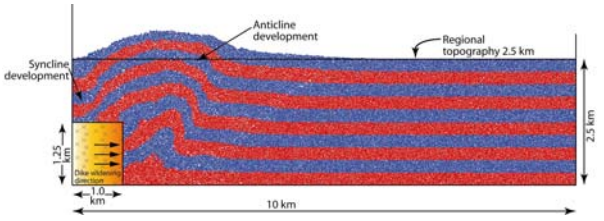

Figure 1. Model A with no bond properties applied to the particles. The red and blue layers are for visualization of deformation and do not reflect any material anisotropy. Final dike width for half-space model is 1 km (2 km total).

Model B was constructed to examine the case of a laterally propagating blade-shaped dike that has reached a

neutral buoyancy level with both the upper and lower dike tips within the model boundaries (Figure 2). The overall dike height is 2.5 km, with 1.25 km of unconsolidated material above and below. The overall deformation style remains consistent with model A: an anticlinal fold develops adjacent to the widening dike producing surface uplift with a syncline developing above the widening dike tip. This deformation all occurs adjacent to and above the dike itself, with little deformation occurring below the lower dike tip. At the surface, the topographic uplift is broader than that produced in model A with a larger fold wavelength generating a wider zone of surface deformation with a similar amount of uplift. The overall effect is a more subtle topographic surface signature than model A.

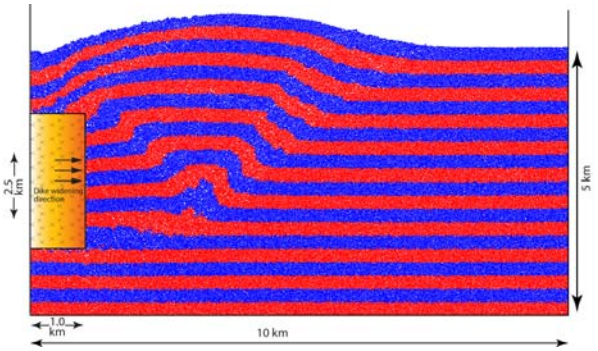

Figure 2. Model B with dike upper and lower dike tips within a 5 km model depth.

For model C, the initial setup is similar to model A, however, the base wall and far right wall of the model boundaries were moved to the right at a rate one quarter of the rate of dike widening (i.e., the dike was widened four times faster than the regional extension applied). Again, overall deformation is accommodated by contractional fold development flanking the widening dike. The effect of regionally extending the model during dike widening is less surface deformation, both in the overall magnitude of uplift and the width of deformation. The extension applied to the model has the effect of creating accommodation space, producing less fold amplification at the surface.

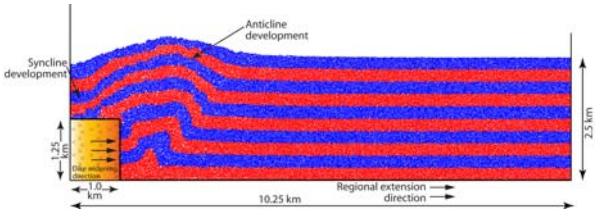

Figure 3. Model C with concurrent regional extension at one-quarter the rate of dike widening.

Implications: In our models, surface deformation took the form of a synclinal trough between two anticlines rather than a graben. Formation of the trough was accomplished primarily through compression adjacent to the dike, causing contractional fold development at the surface. The model evolution indicates that the primary deformation style is via trough margin uplift rather than trough center subsidence and that the most distinctive topographic signature of an underlying dike would be parallel ridges formed by contractional folding on either side of a trough. Variations in dike geometry and the addition of regional extension do not appear to affect the overall style of deformation, but do influence the magnitude of surface deformation, namely producing less uplift and broader zones of deformation.

The Tharsis radial graben systems are characterized by the "simple graben" morphology [13]: long narrow grabens bounded by normal faults, with a down-dropped flat floor unbroken by antithetic faults. Our models of dike widening did not produce this type of simple graben morphology. The primary result of our models was surface deformation in the form of trough development with compressional forces producing uplift at the surface rather than extension over the dike tip producing subsidence. The signature style of dike-induced deformation in this study is contractional folding adjacent to the widening dike. In addition, the volume of subsurface rock that must be displaced to produce this surface deformation is substantial. Evidence for this type of contractional deformation pattern has not been found in terrestrial field analyses or Martian data to date, which suggests that the Tharsis-radial grabens may not have formed solely in response to magmatic dike intrusion.

References: [1] Itasca Consulting Group, Inc. (2002) PFC2D: Itasca Consulting Group, Inc., Minneapolis, Minnesota. [2] Cundall, P.A. and Strack, O.D.L. (1979) *Geotechnique*, *29*, 47–65. [3] Cundall, P.A. (2001) *Geotechnical Engineering*, *149*, 41–47. [4] Potyondy, D.O. and Cundall, P.A. (2004) *Int. J. of Rock Mechanics and Mining Sciences*, *41*, 1329-1364. [5] Schöpfer, M.P.J. et al. (2006) *J. of Structural Geology*, *28*, 816–833. [6] Schöpfer, M.P.J. et al. (2007) *JGR*, *112*, B10401, doi: 10.1029/2006JB004902. [7] Schöpfer, M.P.J. et al. (2007) *JGR*, *112*, B10404, doi: 10.1029/2006JB004903. [8] Wilson, L. and Head, J. (2002) *JGR*, *107(E8)*, doi: 10.1029/2001JE001593. [9] Wyrick, D.Y. and Smart, K.J. (2008) *JVGR*, doi:10.1016/j.jvolgeores.2008.11.022. [10] Rubin, A.M. and Pollard, D.D. (1988) *Geology*, *16*, 413–417. [11] Rubin, A. (1992) *JGR*, *97(B2)*, 1839–1858. [12] Schultz, R.A. et al. (2004) *Geology*, *32(10)*, 889–892. [13] Banerdt, W.B. et al. (1992) Stress and Tectonics on Mars. In: *Mars*. The University of Arizona Press, 249–297.